



Research papers

Temporal patterns in species zonation in a mangrove forest in the Mekong Delta, Vietnam, using a time series of Landsat imagery

Eric L. Bullock^{a,*}, Sergio Fagherazzi^a, William Nardin^b, Phuoc Vo-Luong^c, Phong Nguyen^c, Curtis E. Woodcock^a^a Department of Earth & Environment, Boston University, 685 Commonwealth Avenue, Boston, MA 02215, USA^b Horn Point Laboratory, University of Maryland Center for Environmental Science, Cambridge, MD 21613, USA^c University of Natural Sciences, Vietnam National University, 227 Nguyen Van Cu, dist.1, Ho Chi Minh City, HCMC, Vietnam

A B S T R A C T

Time-series analysis of Landsat imagery was used to evaluate trends in species zonation in a restored mangrove forest in the Mekong Delta, Vietnam. Dating back throughout the primary expansion of the forest, the Landsat archive provides a unique opportunity to examine the evolution of a restored forest in all stages of maturity. Through temporal trend analysis, areas of the forest were divided into four development stages: Pre-mangrove water, initial mangrove colonization, a period dominated by *Sonneratia* spp., and the arrival and zonation of secondary species. Field inventory data was used in conjunction with satellite data to investigate the geomorphic and hydrologic influences behind the species zonation. We hypothesize that the development of *Sonneratia* spp. facilitates initial sedimentation. The trees mature at higher soil elevations and a region develops with low forest density, high light availability, and reduced tidal inundation. Multi-species zonation then develops through the timely exploitation of the geomorphic conditions suitable for the establishment of secondary species.

1. Introduction

Mangrove forests are among the most productive yet vulnerable ecosystems in the world. In coastal habitats, mangroves are essential in erosion prevention, nutrient cycling, and habitat provision. Mangroves are also a vital resource for coastal communities by providing fuel, lumber, fishing grounds, and storm protection (Gebhardt et al., 2012; Vo et al., 2015). Extensive root systems and high concentration of organic matter in the soil allow mangroves to have one of the highest amounts of carbon storage of any ecosystem (Richards and Friess, 2015; Warner et al., 2016). Because of their ecosystem services, the economic value of mangroves is estimated to be in the billions of dollars (Brander et al., 2012).

While mangroves are globally distributed in the tropics between 30°N and 40°S, no other region matches the abundance and variety found in Southeast Asia (Giri et al., 2011). Southeast Asian mangroves are part of a larger grouping of species commonly referred to as 'Old World', or Eastern Hemisphere mangroves. Those in the Western Hemisphere are consequentially referred to as 'New World' mangroves. Southeast Asian mangrove forests exhibit higher levels of species diversity than those in Africa and the Americas, and also have the highest rate of deforestation (Kuenzer et al., 2011; Gebhardt et al.,

2012). From 1950–2000, an estimated one third of the world's mangroves were destroyed, of which almost half occurred in Southeast Asia (Alongi, 2002; Gebhardt et al., 2012). Aquacultural conversion, harvesting for local use, and in some countries war, have all contributed to this dramatic decrease in mangrove forests in the region over the last century.

Mangroves grow in intertidal environments and are often found in distinct zones of individual species (Tomlinson, 1986). While undoubtedly important for ecosystem structure and functionality, the causes of mangrove zonation and distribution are still not well understood (Snedaker, 1982). Currently, the dominant forces thought to control mangrove zonation are succession, geomorphology, external disturbances, ecophysiology, and competition (Lugo and Snedaker, 1974). Early studies utilized ecological succession to explain zonation patterns, with a natural progression from a 'primary' or 'pioneer' species, to one or multiple 'secondary' species (Watson, 1928; Davis, 1940; Tomlinson, 1986; van Loon et al., 2007). However, succession by land building implies that the primary species promotes sediment accumulation and facilitates the arrival of new species, which is not always the case for mangroves. In fact there is evidence that mangroves are merely responding to shoreline progradation without causing it (Thom, 1967). Geomorphology influences the interaction between species develop-

* Corresponding author.

E-mail address: bullocke@bu.edu (E.L. Bullock).<http://dx.doi.org/10.1016/j.csr.2017.07.007>Received 12 September 2016; Received in revised form 28 June 2017; Accepted 17 July 2017
0278-4343/ © 2017 Elsevier Ltd. All rights reserved.

ment and sedimentation. Thom (1967) showed that mangrove species in the Grijalva-Usumacinta Delta in Mexico are segregated according to landform type. Mangrove zonation is thus induced by delta morphodynamics, such as the abandonment of a distributary triggering subsidence or the shifting of the active center of deposition. The influence of landform type is also in part due to the associated changes in hydrodynamics of the landscape, including varying levels of tidal inundation, wave power, and salinity (Woodroffe, 1992). External disturbances include storm surges, extreme winds, droughts, increasing sea level, and anthropogenic influences. Piou et al. (2006) determined that hurricane destruction and subsequent mangrove regeneration was a factor influencing horizontal zonation patterns in Belize. Ecophysiology is based on the physical responses of species to changes in the environment. McKee (1993) indicates that spatial and temporal variations in soil redox potential can affect the distribution of mangrove species. Interspecific competition can also explain mangrove zonation. Cardona-Olarte et al. (2006) showed that some mangrove species have competitive advantage over others within a range of salinity and hydroperiod.

The fast growth and numerous ecosystem services of mangroves have led regions to invest in reforestation efforts over large areas (Lewis, 2005). Restoration projects have had varying levels of success resulting in a range of economic and ecological benefits. While there are often multiple primary objectives, one of the major aims of mangrove restoration is returning to the original levels of biodiversity and ecological functions (Ellison, 2000). Being able to monitor these dynamic systems over large areas would improve our understanding of the processes leading to mangrove zonation as well as improve management and planning of mangrove restoration sites. Restoration sites offer a unique opportunity to study the development of the forest while the zonation is first occurring. This study investigates the use of time-series of remote sensing data to track changes in species zonation of a restored mangrove forest in the Mekong Delta, Vietnam. The same fringe forest was studied by Nardin et al. (2016a, 2016b), who focused on the encroachment of pioneer mangrove species. In this paper we instead study vegetation zonation and the arrival of secondary species.

Through time-series analysis in combination with a high-resolution canopy survey, clear patterns in the expansion and zonation of the forest can be detected. These patterns can then be used to make inferences about the underlying causation of the zonation that has helped the restored forest develop into a mixed-species environment.

1.1. Remote sensing of mangrove forests

The dramatic decrease in the global abundance of mangroves has led to an urgent demand to detect and assess their distribution, composition, and health. Since the locations of mangrove forests are often remote and inaccessible, remote sensing offers the only feasible means of monitoring them over large areas (Kuenzer et al., 2011). Applications of remote sensing for mangrove management can broadly be grouped into two categories. The first category includes attempts to quantify their extent and detect natural and anthropogenic land cover changes. Many of these efforts have utilized high-to-medium resolution optical sensors such as Landsat and SPOT. These sensors offer consistent measurements over time that allow for change detection at spatial resolutions adequate for mangrove classification. The Landsat series of sensors has provided continuous and global data availability at 30-meter spatial resolution since 1982 and 60-meter data since the first launch in 1972. Since then, it has been widely used to assess the distribution (Giri et al., 2011; Long and Giri, 2011) and change in distribution (Béland et al., 2006; Binh et al., 2005; Bui et al., 2013; Dahanayaka et al., 2013; Son et al., 2016; Tran Thi et al., 2013; Tong et al., 2004; Van et al., 2015) of mangroves in Southeast Asia.

The second category includes the assessment of within-stand forest characteristics, such as species composition and nutrient content. There have been a limited number of attempts at mangrove species

mapping in Southeast Asia using Landsat. Myint et al. (2008) used object-based analysis of Landsat imagery for mangrove species classification in Thailand, and Kasawani et al. (2010) tested various spectral indices for use in species delineation in Malaysia. While these studies have demonstrated the feasibility of species classification, the subtle differences in the spectral responses of the different plant traits and unrelated “noise” in the images - such as changing tides - make analysis of specific mangrove traits difficult at this spatial resolution (Gao, 1998).

Time-series analysis is often used to address image quality issues, such as noise and fluctuating tidal water-surface elevation, which inhibit the estimates of vegetation characteristics. By calculating the average trend over time, the day-to-day variability can be removed, and what is left is a clearer signal of what is happening on the ground. Landsat has been widely used for time-series analysis due to its long and continuous data archive (Kennedy et al., 2010; Verbesselt et al., 2010; Zhu et al., 2012). Since time-series analysis utilizes the temporal trajectory of a pixel rather than merely its spectral response, subtle changes or trends can be characterized. This information can give added insight into gradual changes in land cover conditions in addition to reducing classification errors due to image noise.

1.2. Study site

The Mekong Delta is located in the southernmost portion of Vietnam where the Mekong River reaches the sea. The Mekong Delta has a tropical monsoon climate with high precipitation between May and October. The Delta is home to over 17 million people, many of them living in coastal communities (Nguyen, 2007). While the climate is ideal for mangroves, years of war and land conversion have left Southern Vietnam with the highest rates of mangrove deforestation in the country. Recently, the primary driver of mangrove loss has been conversion of land to shrimp aquaculture (Gebhardt et al., 2012). To counteract mangrove destruction, policies were established in the 1980s to begin reforesting the seacoast (San, 1993). Since then, an estimated 1300 km² of mangroves have been reforested (Blasco et al., 2001).

The specific area of interest for our study is a fringe forest on Cù Lao Dung Island at the mouth of the Sông Hậu River. The river is one of the major distributaries of the Mekong River into the South China Sea. The mangrove forest of interest is fronted by a sand and mudflat with the adjacent land being heavily farmed and modified. Between 1993 and 2007 Sóc Trăng Province (where Cù Lao Dung is located) restored 1400 ha of *Sonneratia* (Wyatt et al., 2012). Starting in the 1990's, *Sonneratia* trees were planted at a rate up to of 70 ha per year in Cù Lao Dung, mostly along the southwest forest edge (Wolcke et al., 2015). *Sonneratia* is commonly used as a ‘pioneering’, or introduced species due to its resistance to tropical storms and flooding, ability to grow in high-salinity environments, fast root establishment and growth, and high biomass accumulation (Ren et al., 2008). *Sonneratia* spp. are the natural pioneer species near the distributary mouths of the Mekong Delta, while *Avicennia alba*, *Avicennia marina* and *Rizophora apiculata* are also present along the coast farther from the mouths. The mangrove forest is nowadays considered a healthy ecosystem with high biodiversity (Wolcke et al., 2015).

While regeneration is occurring all along the seaward shoreline, its increase is more noticeable in the southwestern part of the island where the planting effort has been focused. The mangroves are then naturally expanding into areas and during time periods in which no planting is occurring. When geomorphic and ecophysiological conditions allow it, other plants can establish on these mudflats (San, 1993; Li et al., 2012). In addition to an abundance of aquatic species, a large number of insects, such as bees, birds and even macaques (crab eating macaque - *Macaca fascicularis*) live in the mangrove forest. The vast amount of available aquatic species leads to high anthropogenic pressure as people from both Trà Vinh and Sóc Trăng Provinces travel

to Cù Lao Dung to collect clams and crabs.

Fricke et al. (in this issue) found sedimentation patterns in Cù Lao Dung to be dependent on season, with increased offshore sediment deposition occurring during the southwest monsoon season (July to December). In the following dry season, a decrease in water discharge from the rivers results in a mangrove-directed flux of water and suspended sediments from the ocean (Eidam et al., in this issue). In our discussion we hypothesize that species colonization in the mangrove forest of interest follows the seasonal deposition of sediments and resulting land progradation. This development pattern would follow the theory that species zonation is controlled by timely exploitation of suitable conditions for survival (Thom, 1967). In our study area, as is common in the region, *Nypa fruticans*, *Avicennia* spp., and *Aegiceras corniculatum* can be found at higher elevations (San, 1993). Despite human assistance in the plant establishment, the species distribution provides similar ecological functions as a natural forest (Wolcke et al., 2015). To better understand the processes influencing mangrove forest development, more information is needed on the causes and timing of species zonation. Since the restoration of the study area began in the 1980s, we are offered a unique opportunity to study zonation dynamics during the major expansion of the forest through satellite imagery.

2. Methods

2.1. Field campaign

Field inventory data were collected in March 2015. Vegetative traits were collected along two transects perpendicular to the fringe. The transects were chosen based on accessibility and vegetative diversity. Data were collected every 30 m along the transects. To measure tidal elevations and flooding duration two Nortek Aquadopp Doppler Current Profilers (ADCP) were deployed at locations 4 and 25 (Fig. 1). The Aquadopp at location 4 recorded water elevation every ten minutes from 22 to 9-2014 to 3-10-2014 and from 3 to 3-2015 to 13-3-2015. The Aquadopp at location 25 recorded water elevation every ten minutes from 23 to 9-2014 to 4-10-2014 and from 4 to 3-2015 to 15-3-2015. From the time-series of tidal elevation we derived the Mean High Water elevation for both location 4 and 25. Relative elevations along the two transects were measured using a Topcon GTS

252 Total Station and referenced to Mean High Water utilizing the tidal data collected by the ADCPs. The tidal data in conjunction with elevation data allowed us to determine the average flooding period (minutes per day) for several points along Transect 1 and 2 (see also van Loon et al., 2007).

A forest survey (number of trees and diameters at breast height) was conducted in a 10 m circular radius every 30 m along the transect. The dominant species at the survey points were assigned based on the species with the highest number of individuals present within a radius of 10 m from the transect points (Table 1). Stem density was chosen as the parameter of interest for a few reasons. First, *Sonneratia* spp. was found to be the species with highest basal area for almost all the sample points, likely due to *Sonneratia* spp. having been planted throughout the forest. Any spatial patterns in remote-sensing reflectance can therefore be inferred to be more responsive to changing complexity of the forest in terms of species composition than changes in biomass. Additionally, the study aims to investigate the patterns of species distribution and is thus limited to any conclusions about additional vegetation properties. Two sample points that were not dominated by any single species were removed from the analysis. A few sites located around 3 km away from the two transects were also sampled to characterize the area farthest from the river channels and to better capture the spatial variability of the forest (samples 34 and 35; see Fig. 1 and Table 1).

2.2. Spatial analysis based on Landsat images

All Landsat 4, 5, 7, and 8 images for WRS-2 Path 125 Row 053 were processed to surface reflectance using the LEDAPS atmospheric correction algorithm and downloaded from the EROS Science Processing Architecture along with the Fmask cloud and cloud shadow mask (Masek et al., 2012; Zhu and Woodcock, 2012). The images were then transformed into corresponding Brightness, Greenness, and Wetness (BGW) images based on the Tasseled Cap transformation for surface reflectance proposed in Crist (1985). BGW units are henceforth presented in transformed Tasseled Cap components $\times 10,000$. The BGW values for the sample points in Table 1 can be seen in Fig. 2.

For reference purposes, a species map was created for the time of the survey. The dominant-species labels for the field survey points were

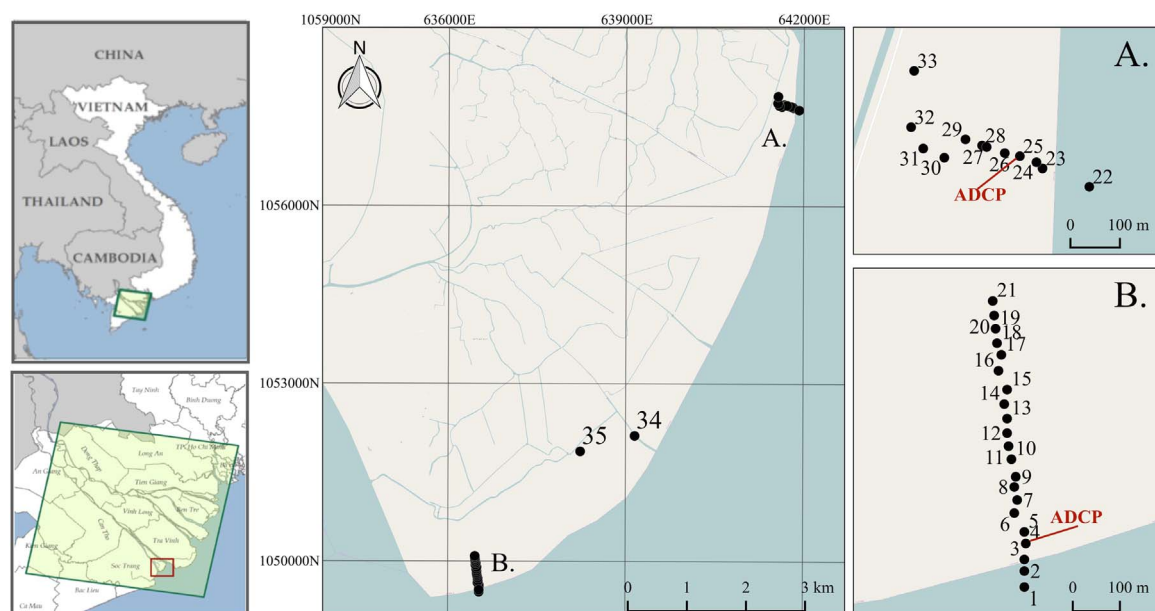


Fig. 1. Left: Mekong Delta, Vietnam. The study area is indicated in the red box and corresponding Landsat scene in green box (adapted from Nardin et al., 2016a). Center: Sample locations for Transect 1 (A.) and 2 (B.) Right: Zoomed-in view of both transects with ADCP locations labeled at sample points 4 and 25. (For interpretation of the references to color in this figure legend, the reader is referred to the web version of this article.)

Table 1

Species count for the sample locations. Asterisk denotes samples removed due to a lack of species dominance. Double asterisk denotes samples shown in Fig. 5.

Sample #	Trees per Ha				Basal Area (m ² /Ha)			
	<i>Sonneratia</i> spp.	<i>Aegiceras corniculatum</i>	<i>Avicennia</i> spp.	<i>Nypa fruticans</i>	<i>Sonneratia</i> spp.	<i>Aegiceras corniculatum</i>	<i>Avicennia</i> spp.	<i>Nypa fruticans</i>
1	2580	0	0	0	6.25	0	0	0
2	955	0	0	0	3.12	0	0	0
3	924	0	0	0	4.52	0	0	0
4	541	0	0	0	3.20	0	0	0
5	478	0	0	0	6.72	0	0	0
6**	573	0	0	0	6.58	0	0	0
7	414	0	0	0	5.02	0	0	0
8	382	32	0	0	2.50	< .001	0	0
9	382	32	0	0	4.77	< .001	0	0
10	255	64	0	0	2.46	< .001	0	0
11	446	0	0	32	3.85	0	0	0.01
12	255	32	0	0	3.54	< .001	0	0
13	318	32	0	32	2.77	< .001	0	0.01
14	255	159	96	64	3.92	< .001	0.35	0.03
15	541	96	0	127	3.81	0.01	0	0.22
16*	605	318	0	255	3.94	0.01	0	0.61
17*	732	446	32	382	4.46	0.05	< .001	0.57
18	446	32	0	541	4.42	0.06	0	1.58
19	350	64	0	478	2.77	0.01	0	2.35
20	127	32	0	541	1.24	0.01	0	1.86
21**	127	0	0	605	2.31	0	0	2.21
22	32	0	0	0	1.03	0	0	0
23	64	0	0	0	8.66	0	0	0
24	32	0	0	0	10.12	0	0	0
25	64	0	0	0	1.03	0	0	0
26	191	0	0	0	2.84	0	0	0
27	382	0	0	0	3.22	0	0	0
28	255	3662	32	0	2.76	0.25	1.59	0
29	414	2548	0	0	2.74	0.38	0	0
30	223	3981	0	0	2.68	0.52	0	0
31**	127	3312	318	0	2.74	0.98	0.19	0
32	191	1752	605	0	4.97	0.72	0.51	0
33	159	860	2070	0	2.08	0.20	1.71	0
34	191	1019	924	127	3.32	0.09	1.05	0.06
35**	127	0	1115	223	0.86	0	3.42	0.47

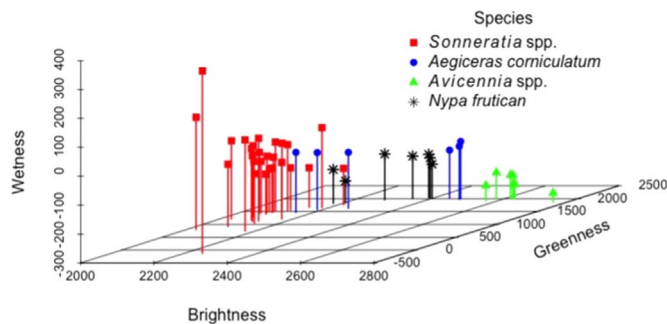


Fig. 2. Mean Brightness, Greenness, and Wetness values in March 2015 classified by dominant species within each pixel area.

used as inputs to a Random Forests classifier for species classification in 2015. The classifier was trained and applied to a 2015 mean BGW image using the *Orfeo ToolBox version 5.2* (2015). Only Landsat 8 images (seven, in total) were used to calculate the mean BGW values. The year 2015 was used to correspond with the time of the field survey. The images used were collected between January and August.

Although we believe the classification to closely resemble the patterns of the species from the field campaign, the 4-species map cannot be statistically validated due to inadequate reference imagery to accurately differentiate the species. Since the focus of the study is to investigate the factors leading to the prominence of species other than *Sonneratia*, an accuracy assessment was performed based on two classes: *Sonneratia* spp. and non-*Sonneratia*. This assessment was made possible by the differentiability of *Sonneratia* from the other species in high-resolution optical imagery (Fig. 3). For the validation

we used a very high spatial resolution aerial image of the fringe forest collected on January 25th, 2015 (Astrium, courtesy [Google Earth, 2016](#)). From the categorized map we created a stratified random sample for the *Sonneratia* and secondary species classes (50 pixels for *Sonneratia*, 50 pixels for the secondary species). We then conducted a visual assessment of the vegetation present in each 30 × 30 m² pixel after projecting the sample pixels on the aerial photograph. Photographs from the field campaign were used to aid in the distinction between the two classes. Although some samples likely contained a mixture of species including *Sonneratia* and non-*Sonneratia*, they were assigned to the class they appeared to most closely represent. If they appeared to be evenly mixed, or a class label could not be confidently determined, then the sample unit was removed from analysis. Accuracy metrics from the visual assessment are outlined in [Table 2](#).

2.3. Temporal analysis with Landsat Images

Brightness, Greenness, and Wetness time-series were compared visually to see if there were patterns that helped differentiate among species. Smoothing splines were fit to the Brightness, Greenness, and Wetness values for each pixel over time. The smoothing was done to reduce the day-to-day variability resulting from missed clouds and other noise in the images and represents the overall trend through time. Monthly predictions of Brightness, Greenness, and Wetness were made from 1990 until 2015 based on the spline fits (Fig. 4). The temporal trajectories were then separated into distinct time segments according to their vegetative state.

The separation between species was found to be predominately

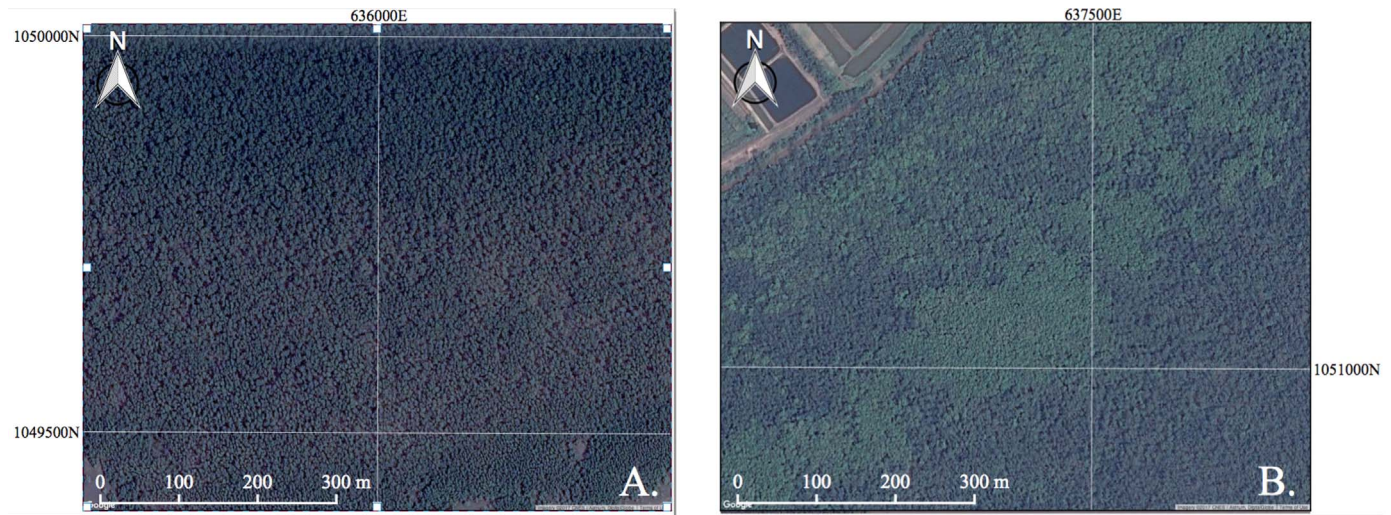


Fig. 3. High-resolution optical imagery for A. *Sonneratia* and B. A mixture of *Avicennia* and *Aegiceras corniculatum*.

Table 2

Result of 100-sample accuracy assessment. Average user's, producer's, and overall accuracy: 95.02%, 95%, and 95%.

Reference		<i>Sonneratia</i>	Non- <i>Sonneratia</i>	Total	Producers' Acc. (%)
Map	<i>Sonneratia</i>	48	2	50	96.00
	Non- <i>Sonneratia</i>	3	47	50	94.00
	Total	51	49	100	
	User's Acc. (%)	94.11	95.92		

based on their Greenness. It should be noted that in Fig. 2, the Greenness axis spans a much greater range than the other two. Additionally, the time segments were found easiest to classify using the Greenness time-series, in which *Sonneratia* and mixed-species or non-*Sonneratia* pixels could be differentiated for both transects based on the difference in Greenness between the minimum after colonization and at the end (Fig. 4). The difference in Greenness metric is defined as:

$$G_{\text{dif}} = G_{\text{end}} - G_{\text{min}} \quad (1)$$

where G_{dif} is the difference in Greenness, G_{end} is the Greenness at the end of the time-series based on spline prediction, and G_{min} is the minimum Greenness after colonization based on spline prediction.

Fig. 5a illustrates data from a sample pixel that is located near the fringe of the forest in a stand of *Sonneratia* that established around 2005, 5b and 5c are from zones of *Aegiceras corniculatum* and *Nypa*

fruticans in the middle of the forest and established around 2000, and 5d is from farthest inland in a patch of *Avicennia* spp. that established around 1996. The trajectory of each pixel was divided into temporal segments corresponding to the following conditions: pre-mangrove water, initial colonization, a period with only *Sonneratia* spp. present, and the introduction/presence of secondary species. The first segment consists of a Greenness value under a mangrove threshold of 700 and represents the time period before the pixel made the transition from tidal flat to forest (Fig. 5a). The threshold was found through manual interpretation of the mean 2015 Greenness image at the forest fringe in conjunction with a 2015 high-resolution image from Google Earth. The threshold was gradually increased until all visible mangroves were included. The second segment represents initial colonization of *Sonneratia* (Fig. 5d), characterized spectrally by a spike in Greenness. In the third time segment the Greenness drops substantially (G_{min} in Fig. 5b). If there had been the introduction of a secondary species there will be a final segment with a long and gradual increase in Greenness (rising to G_{end} in Fig. 5b; see upward trend in Greenness labeled in 5d).

Some additional classification rules were applied to reduce misclassification of the time segments. Pixels that have a Greenness below 1500 at the end of the time-series are classified as *Sonneratia*. This threshold was chosen based on the Greenness values for the sites in the field transects, in which no location dominated by *Sonneratia* was above 1500 in the 2015 image. To avoid misclassifying newly established *Sonneratia* saplings at the tidal flat-forest boundary that are especially Green, pixels with a G_{dif} value under 500 were not considered candidates for the *transition* class. All pixels that passed those conditions in time were mapped as having transitioned from

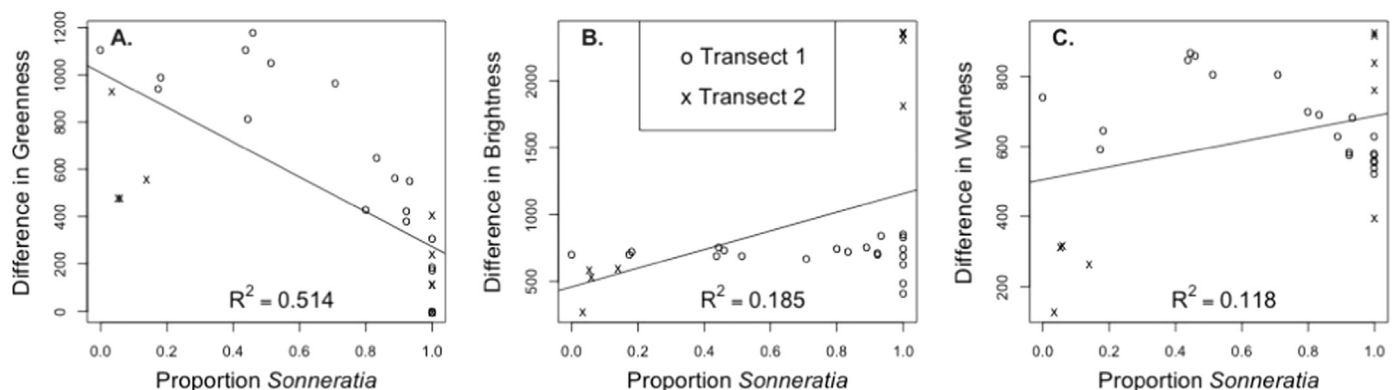


Fig. 4. Linear regression models based on the difference in Greenness (A), Brightness (B), and Wetness (C) from the minimum after colonization to the end of the time period.

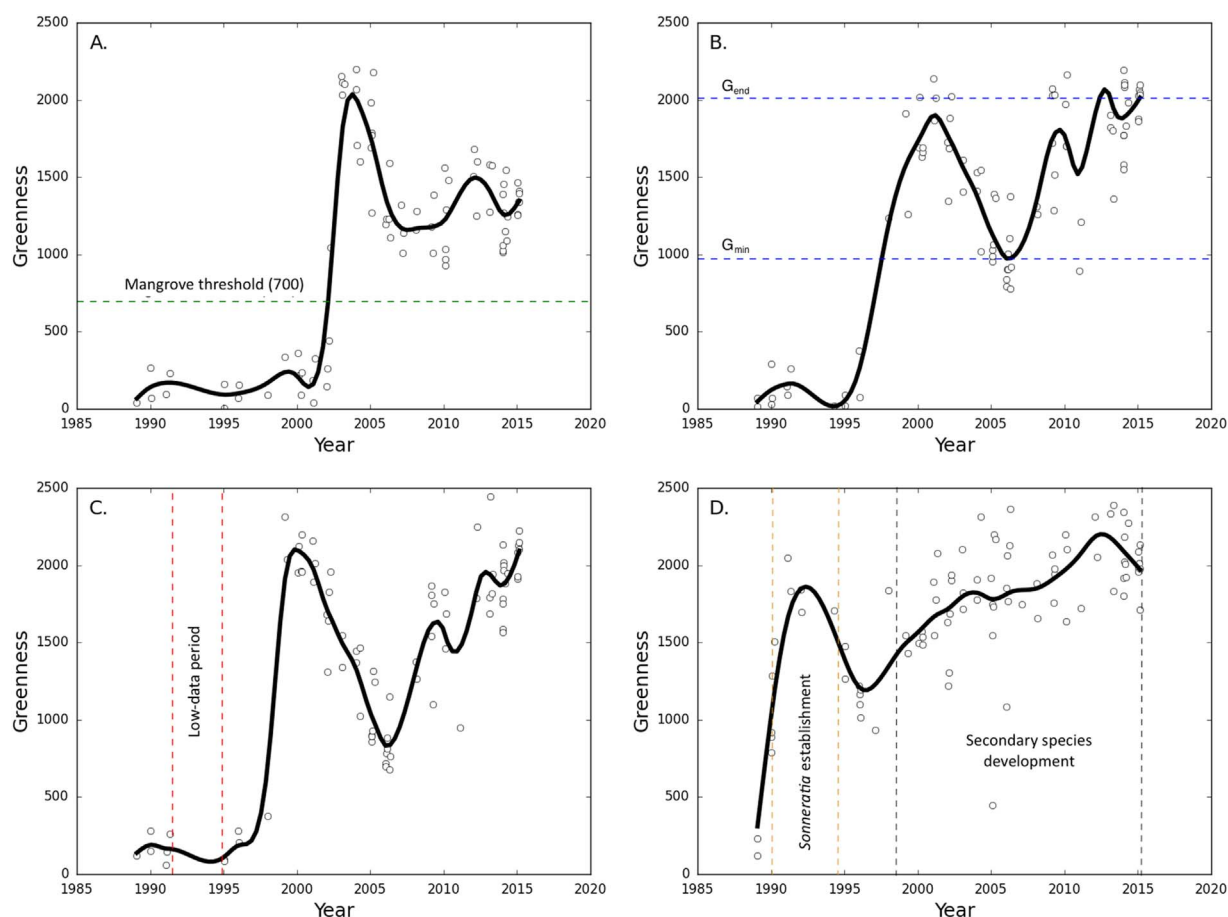


Fig. 5. Temporal trajectory of Greenness values for four pixels indicated in Table 1. Point A) is currently dominated by *Sonneratia*, B) by *Aegiceras corniculatum*, C) by *Nypa fruticans*, and D) by *Avicennia*. The temporal segments used for mangrove-state classification are labeled for the threshold distinguishing mangroves from non-mangroves (A.) and the G_{\min} and G_{end} metrics used to calculate G_{diff} and distinguish final species type (B.). Additionally labeled is the period of low-data density labeled in Fig. 8(C.) and the periods of *Sonneratia* establishment and secondary species development (D.). (For interpretation of the references to color in this figure, the reader is referred to the web version of this article.)

Sonneratia to other species.

3. Results

3.1. Spatial analysis

As seen in Fig. 2, the four species can be differentiated in the 3-dimensional BGW space. *Avicennia* is separated from the other vegetation by its high Brightness values, while *Sonneratia* is separated based on its low Greenness and Brightness and high Wetness. *Aegiceras corniculatum* and *Nypa fruticans* display high Greenness and intermediate Wetness and Brightness. The difference in BGW components provides the basis for attempting to map the distribution of all four species at the time of the field campaign (Fig. 6), and calculate a two-class error matrix (*Sonneratia*, secondary species) with estimates of accuracy (Table 2). The classification yields an overall accuracy of 95%, with a user's accuracy between 94% and 96% and a producer's accuracy between 94% and 96%.

The fringe of the forest is completely dominated by *Sonneratia*, with other species dominating the inland portion of the forest. On the inner-western side, *Nypa fruticans* is present, while *Aegiceras corniculatum* has developed on the inner-eastern side, and can be found between the *Sonneratia* and *Nypa fruticans* zones on the western edge. In the middle and inner areas small patches of *Avicennia* can be found. It should be noted that in some areas classified as *Sonneratia* the non-*Sonneratia* species were also present, so Fig. 6 does not fully represent the dynamic nature of the forest. Additionally, the overlap in BGW values for *Aegiceras corniculatum* and *Nypa fruticans* likely resulted

in some misclassification in those two classes. Despite this, the patterns in the map closely resemble the field observations and the plot data (Table 1).

Moving inland along Transect 1, Greenness is high at the water boundary and then decreases with increasing elevation. After reaching a minimum when *Sonneratia* spp. is still dominant, Greenness continuously increases with elevation, as does the presence of other species (Fig. 7a). The elevation gradually rises, and more individuals of *Nypa fruticans* and *Aegiceras corniculatum* are present. For both transects the *Sonneratia* basal area remains relatively constant, with an exception being a large increase near the fringe in Transect 2 due to a few very large trees. The average inundation duration is lower along Transect 1, starting at 574 min/day 90 m from the boundary between forest and tidal flat and decreasing to 271 min/day at the end of the transect (Fig. 7). Transect 2 has lower elevations, so that at 60 m from the forest seaward boundary the average inundation period is 902 min/day while at the end of the transect it is 563 min/day (Fig. 7). As a result the encroachment of secondary species occurs at different inundation duration in each transect: 376 min/day in Transect 1 and 708 min/day in Transect 2.

3.2. Temporal analysis

3.2.1. Transition from tidal flat to mangroves

The expansion of the mangroves occurred earlier in the study period in the area closer to the distributaries (Fig. 8a). More recently, the middle area began to fill. In a previous study in the same forest, Nardin et al. (2016a) found the fringe to be expanding around 30 m/yr

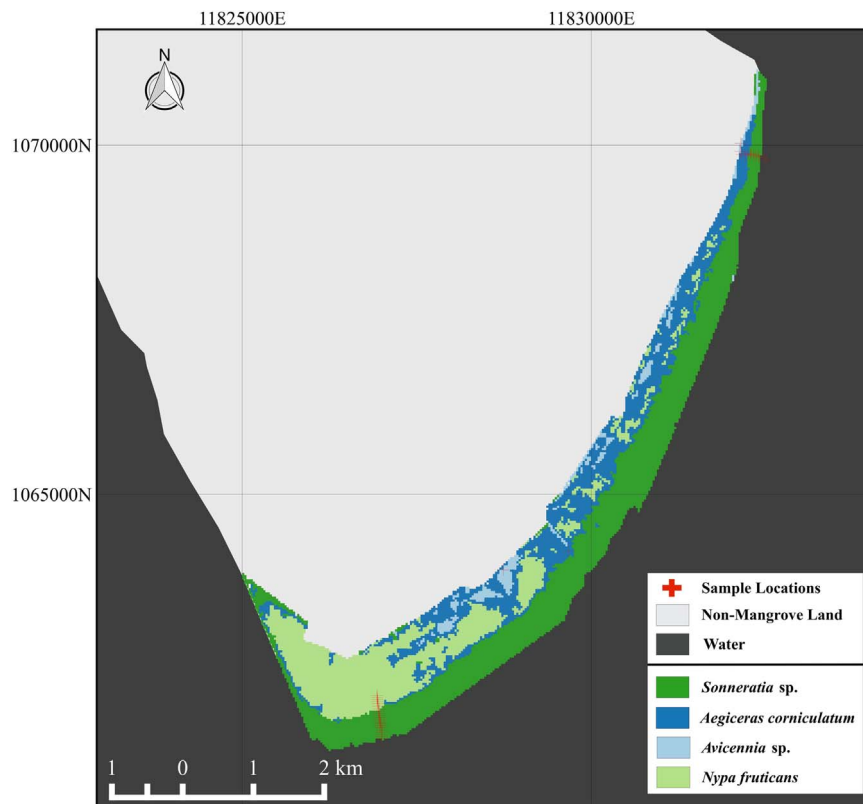


Fig. 6. Mangrove species classification using mean Brightness Greenness Wetness values in 2015.

from 1995 to 2005, which was the peak of the expansion period. The encroachment of *Sonneratia* is very consistent in the southwest and northeast parts of the fringe, while it is patchy in the fringe center. The gradual expansion in mangrove colonization is consistent with ^{210}Pb geochronology records reported in Fricke et al. (in this issue). The century-scale sediment records show a gradual sedimentation of 3–5.1 cm/yr over the period of our study, which, considering a measured slope of 0.001 for this part of the forest, yields an average progradation rate between 30 and 50 m/yr.

3.2.2. Primary mangrove species versus secondary mangrove species

By looking at the difference in Greenness between the minimum of the time-series and the end of the time-series, it can be seen that there is clearly a spatial pattern, with inland areas having a much greater difference between minimum and end-of-time-series Greenness (Fig. 9b). The exception is a patch of *Aegiceras corniculatum* in the southwest region of the forest (circled area in Fig. 9b), in which the difference in Greenness is low. The minimal difference is likely influenced by a data gap period in the Landsat archive during the early 1990s, shortly after the area was colonized (see red lines in Fig. 5C). Therefore, because of lack of images, we likely missed the dip in Greenness exhibited elsewhere.

The timing of the modeled establishment of secondary species is clearly concentrated in the final months of the calendar year (October to December), corresponding to the end of the rainy season (Figs. 8b, 10). It appears that the encroachment occurs over large swaths of forest in short periods followed by long periods without expansion of secondary species.

4. Discussion

4.1. Stages of mangrove development

By comparing the spectral and temporal characteristics of different

mangrove species, it can be seen that there are clear patterns to the development of a mangrove forest in a prograding delta. The development of a stand of mangroves is in fact divided in stages that can be seen in the fringe studied herein. Sediment washed offshore during the rainy season accumulates at the shore during the more energetic conditions of the dry season, therefore increasing elevations and promoting the expansion of *Sonneratia* spp. This expansion can be seen in a large jump in Greenness in the Landsat data in the area that the *Sonneratia* first develops. After original colonization there is a period of high basal area but low plant density as the *Sonneratia*-dominated forest is maturing. This period corresponds to low Greenness in the remote sensing observations. As the bed elevation gradually rises there is an establishment of secondary species with total basal area drastically decreasing and Greenness sharply increasing.

4.2. Possible contributing factors

A possible explanation of the observed decline in dominance by *Sonneratia* is tree burial and root smothering due to sediment accumulation. Fricke et al. (in this issue) measured very high sedimentation rates in the interior of the southwest fringe (5.1 cm/yr) that would possibly negatively affect the young and vulnerable mangrove trees. Note that the sedimentation rates measured by Fricke et al. (in this issue) in the tidal flats in front of the forest are lower (3.0 cm/yr), suggesting that the mangroves facilitate sediment deposition.

Another possible explanation for the increase in light availability, the reduction in forest density, and the slight decrease in *Sonneratia* basal area along the southwest transect is a change in inundation regime. van Loon et al. (2007) indicate that *Sonneratia* spp. are adapted for a duration of inundation between 400 and 800 min/day. In the southwest transect, secondary species are first found in the forest when the duration of inundation is less than 380 min/day (Fig. 7), which is not favourable for *Sonneratia*. The duration of inundation would also explain why seedlings are absent at the northeast forest-sea

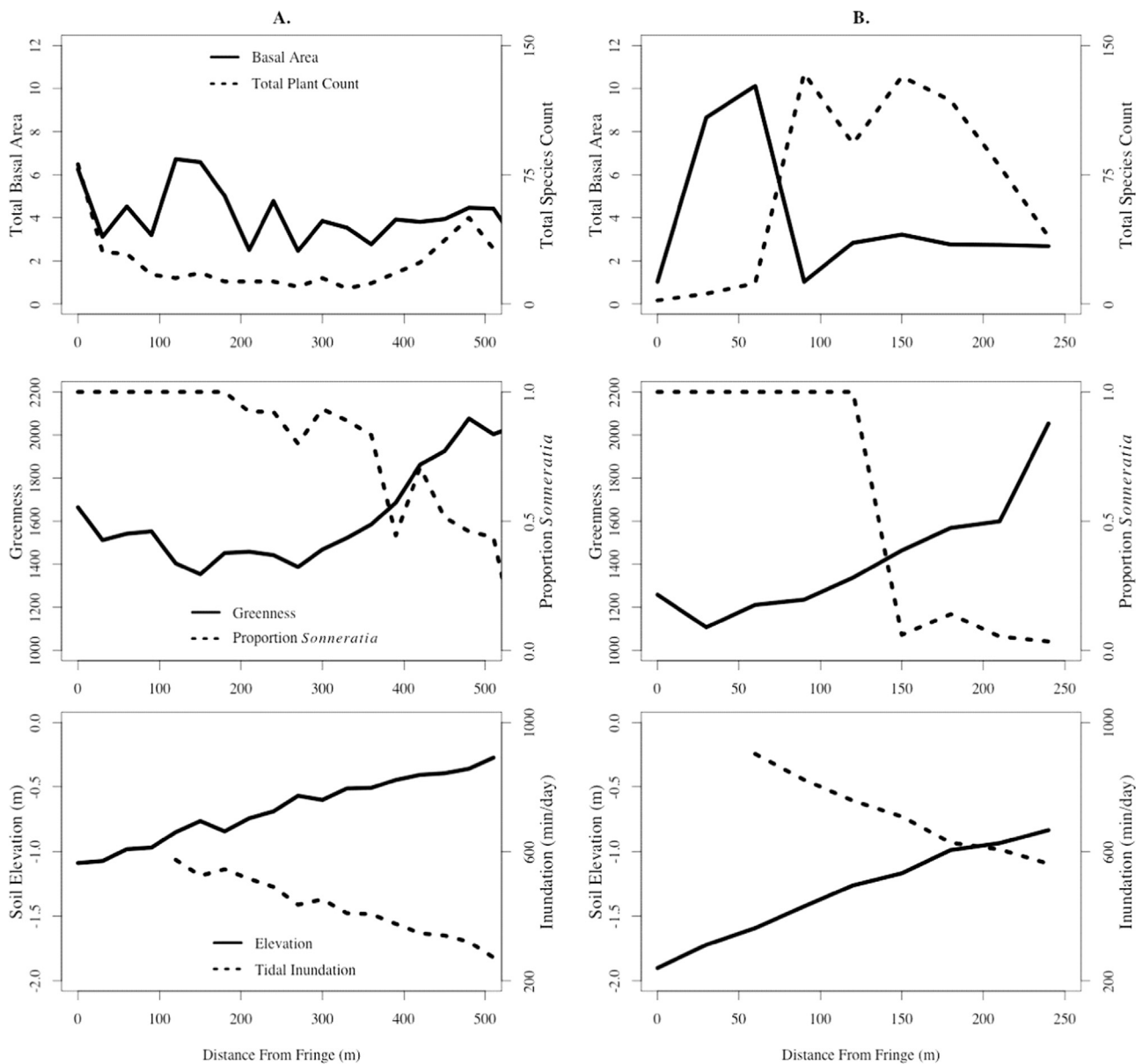


Fig. 7. A) Total plant basal area and count (top), Greenness and proportion *Sonneratia* (middle), and elevation and tidal inundation (bottom) compared to distance from the tidal flat-forest boundary along (A) Transect 1 and (B) Transect 2. See Fig. 1 for location.

boundary. Here bottom erosion increased the duration of inundation above 900 min/day, above the limit indicated by van Loon et al. (2007). Large trees might be able to survive these longer inundation periods but the forest is unable to recruit new seedlings.

As a result of all these factors, in the area between the fringe and inland region of the forest (samples 10–13, 25–27 in Table 1) Nardin et al. (2016b) measured a lower forest density, gaps in the forest canopy, higher light availability, and absence of *Sonneratia* seedlings. In this area new seedlings do not establish as extensively and the existing trees are larger in diameter. Our new research shows that this pattern is consistent with the Greenness and G_{dif} patterns in the remote sensing observations. It is likely that in areas of low forest density and high light availability, the reflectance in the remote sensing data consists of a higher proportion of understory and water. Where the canopy is denser, as in the forest fringe and inland, the reflectance corresponds almost entirely to the vegetated canopy cover. Therefore, the Greenness is higher in more dense areas of the forest. Our hypothesis is that higher elevations developed from sediment deposition, combined with reduced forest density, diminishing interior wave

intensity and increased light availability in these areas are adequate conditions for new and non-*Sonneratia* species establishment. This hypothesis supports the concept that mangrove zonation is due to a timely exploitation of geomorphic conditions suitable for survival (Thom, 1967).

4.3. Species-level patterns

Balke et al. (2011) showed that many mangrove species require a disturbance-free time period to establish roots. Once the seedlings are established, they need time to grow long enough to withstand waves and strong currents. When studying our same area, both Henderson et al. (in this issue) and Norris et al. (in this issue) found wave dissipation to be enhanced by high pneumatophore density in the fringe stands of *Sonneratia*. The buffer from wave energy provided by the densely populated *Sonneratia* on the fringe likely favors the establishment of other mangrove species in the interior of the forest. Therefore enhanced wave dissipation is another benefit of using *Sonneratia* as a pioneering species during restoration.

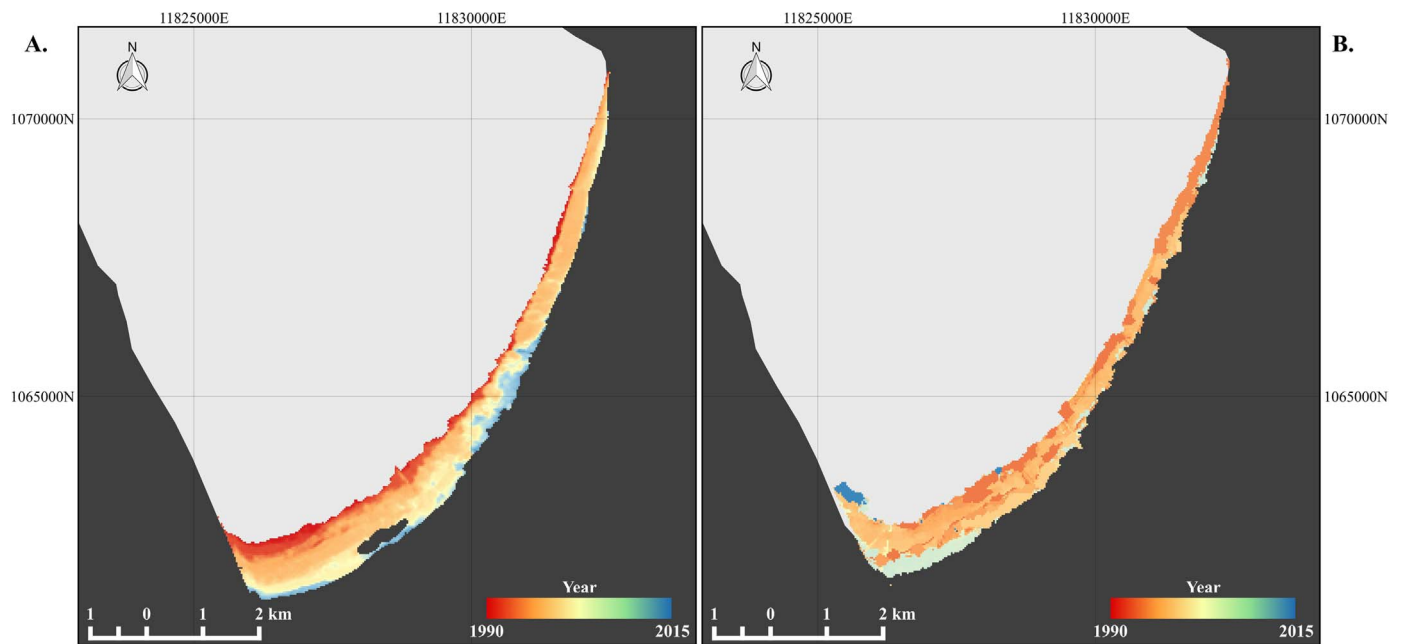


Fig. 8. A) Year of *Sonneratia* species arrival; B) year of minimum Greenness after the arrival of *Sonneratia*, indicating the encroachment of secondary species.

For *Aegiceras corniculatum*, Liao et al. (1998) found that a mudflat elevation of at least 1.42 m above the mean tidal plane is ideal for survival. During our field campaign *Aegiceras corniculatum* was first found at much lower elevations: 0.85 m meters above the mean tidal plane for Transect 1 and 0.12 m for Transect 2, assuming a tidal range of 2.59 m. This discrepancy indicates the need to use inundation duration, which depends on tidal range, rather than bottom elevation to study vegetation zonation in mesotidal environments, as indicated by van Loon et al. (2007).

Moreover, the difference in flooding duration at the location of secondary vegetation encroachment shows the importance of the geomorphic evolution of the site. In a fast prograding setting like Transect 1, secondary species might not have had time to encroach the

lowest elevations, while in a slowly prograding or eroding area like the one near Transect 2 *Aegiceras corniculatum* thrives much lower in the tidal frame. These individuals probably established in the past when the bed elevation was higher, and are still able to survive the increase in flooding duration caused by the erosion of the bottom. Another possible explanation is that *Aegiceras corniculatum* cannot withstand the high sedimentation rates of the southwest fringe. Our data therefore supports the importance of ecogeomorphic factors in the development of mangrove forests in dynamic landscapes.

4.4. Timing of secondary species development

Looking at the species distribution at the end of the time-series, it

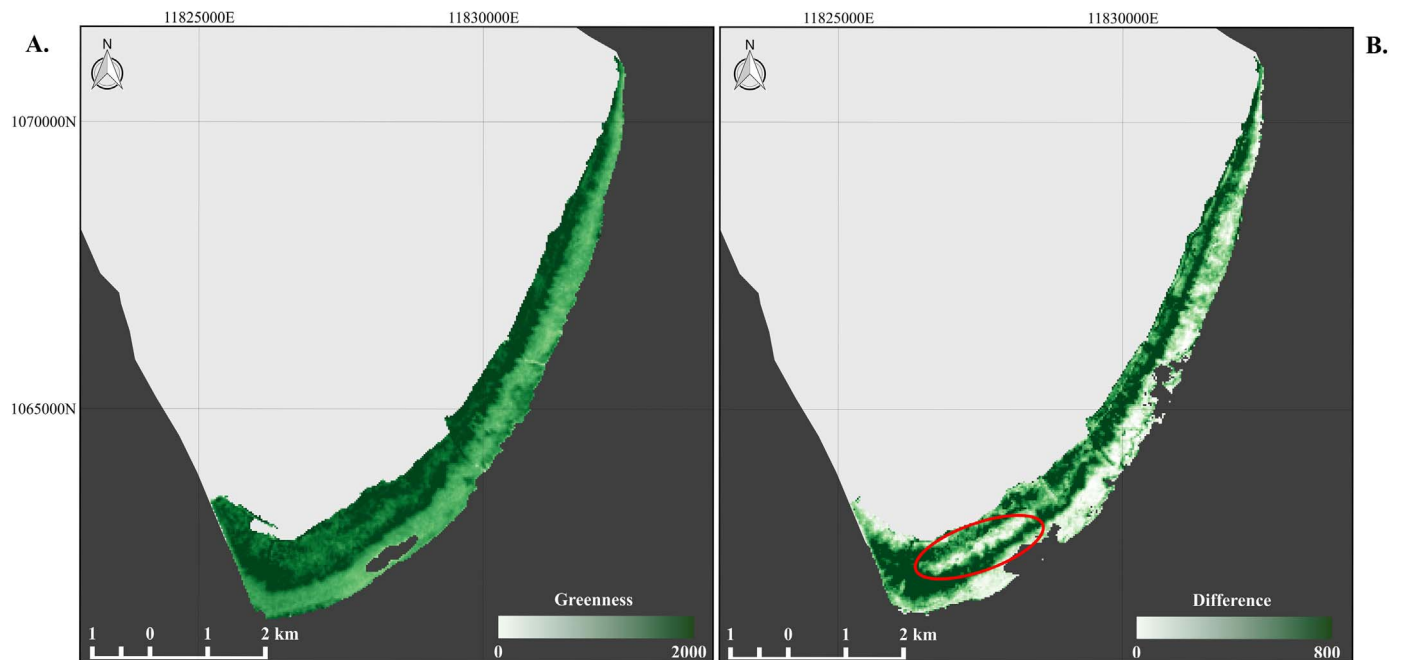


Fig. 9. A) Average Greenness in 2015 and B) difference between minimum Greenness after colonization and Greenness at the end of the time-series. The area circled in red is affected by a data gap in the Landsat archive and should not be considered (see ‘Temporal Analysis’ section of text for details). (For interpretation of the references to color in this figure legend, the reader is referred to the web version of this article.)

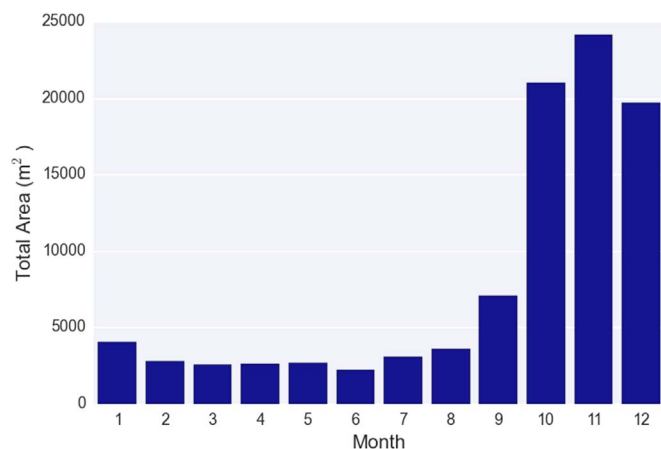


Fig. 10. Total area of secondary species establishment as a function of month of arrival.

can be seen that the transition from *Sonneratia* to other species does not occur homogeneously (Fig. 8). The western side of the forest exhibited high mangrove expansion and sedimentation, and a stand of mostly *Nypa fruticans* in the inner portion. The eastern side saw less sedimentation and resulting outward expansion, and is now composed of a mix of *Avicennia* spp. and *Aegiceras corniculatum* above the *Sonneratia* boundary. This difference is likely influenced by the amount of freshwater discharged by the distributaries on each side of the restored forest and by the different duration of inundation. In fact, past research has shown that *Nypa fruticans* is sensitive to high salinity, and will usually thrive in areas of fresh to brackish water (from 0 ppt to 10 ppt) that only rarely experience tidal inundation (Robertson et al., 1991; Marchand, 2008). Fricke et al. (in this issue) found the salinity in the forest to be lower during the rainy season due to an increase in freshwater discharged from the river. Additionally, Fricke et al. (in this issue) found the peak salinity to be higher in the northeast portion of the forest (23 ppt during spring tides in the dry season) but maximum wave energy to be higher in the southwest. The high salinity and the longer flooding duration likely inhibits the establishment of *Nypa fruticans* in the northeast fringe (Fig. 6). Since the timing of the secondary species arrival corresponds to the months between the wet and dry seasons, it is likely that the period of reduced salinity aids in the development of the less-halotolerant secondary species. More research for the specific species regarding wave and salinity tolerance during the development phase and responses to seasonal changes in hydrologic conditions is needed to validate our results.

4.5. Study limitations

There are some considerable limitations to the model presented that should be addressed. First, the availability of Landsat data varies through time and is concentrated in the less rainy months. Data gaps due to sensor failures or changing acquisition strategies can create years in which no images are available (Figs. 5 and 9). Secondly, the observed relationship between Greenness and species density ignores additional forest characteristics such as biomass, leaf area index, or canopy cover. These complexities are likely to influence the Greenness of the forest beyond simply the species composition. This limitation is likely causing the steep drop in the proportion of *Sonneratia* seen in Fig. 7b, during a time of only moderate Greenness increase.

5. Conclusion

With the complexity of mangrove ecology and noisiness of the remote sensing images in the regions where they are found, the combined use of both satellite and field data is needed to accurately monitor mangrove development. Detailed monitoring is especially

important in restoration sites, where biodiversity and growth is often essential for the forest's survival. Here we suggest an approach that utilizes a time-series of remote sensing data in conjunction with hydrologic, vegetation, and geomorphic field data to better understand the development of mangrove forests.

The findings presented here support the hypothesis that morphodynamics control the hydrological and ecological conditions necessary for a multi-zoned mangrove forest to develop. The *Sonneratia* on the forest fringe support the habitable conditions for the transition into a mixed-species forest. While the manual planting of the mangroves on bare tidal flats and then natural expansion of the pioneer species is relatively continuous, the arrival of secondary species is intermittent, with large areas colonized in short time periods. The secondary species arrival corresponds to the timing of seasonal sediment delivery to the shoreline and occurs in areas of low wave energy, low forest density, increased elevation, and reduced tidal inundation. It can therefore be stated in the studied forest that secondary species arrival occurs due to the timely exploitation of hydrologic and geomorphic conditions that in turn influence the zonation patterns occurring thereafter.

Acknowledgements

This research was supported by the by the ONR award N00014-14-1-0114 in addition to the USGS Landsat Science Team Program for Better Use of the Landsat Temporal Domain: Monitoring Land Cover Type, Condition and Change (grant number G12PC00070). We would like to thank Richard Nguyen, Daniel Culling, Aaron Fricke and Charles Nittrouer for the logistical support during fieldwork. We are also grateful for the USGS Earth Resources Observation and Science Center for the Landsat surface reflectance data. Finally, we thank the Scientific Python and R communities in addition to Google and the Centre National D'études Spatiales (CNES) for the development and distribution of the software essential for our analysis.

References

- Alongi, D.M., 2002. Present state and future of the world's mangrove forests. *Environ. Conserv.* 29, 331–349. <http://dx.doi.org/10.1017/S0376892902000231>.
- Balke, T., Bouma, T.J., Horstman, E.M., Webb, E.L., Erftemeijer, P.L.A., Herman, P.M.J., 2011. Windows of opportunity: thresholds to mangrove seedling establishment on tidal flats. *Mar. Ecol. Prog. Ser.* 440, 1–9. <http://dx.doi.org/10.3354/meps09364>.
- Béland, M., Goita, K., Bonn, F., Pham, T.T.H., 2006. Assessment of land-cover changes related to shrimp aquaculture using remote sensing data: a case study in the Gao Thuy District, Vietnam. *Int. J. Remote Sens.* 27, 1491–1510. <http://dx.doi.org/10.1080/01431160500406888>.
- Binh, T.N.K.D., Vromant, N., Hung, N.T., Hens, L., Boon, E.K., 2005. Land cover changes between 1968 and 2003 in Cai Nuoc, Ca Mau Peninsula, Vietnam. *Environ. Dev. Sustain.* 7, 519–536. <http://dx.doi.org/10.1007/s10668-004-6001-z>.
- Blasco, F., Aizpuru, M., Gers, C., 2001. Depletion of the mangroves of continental Asia. *Wetl. Ecol. Manag.* 9, 245–256. <http://dx.doi.org/10.1023/a:1011169025815>.
- Bui, T.D., Maier, S.W., Austin, C.M., 2013. Land cover and land use change related to shrimp farming in coastal areas of Quang Ninh, Vietnam using remotely sensed data. *Environ. Earth Sci.* <http://dx.doi.org/10.1007/s12665-013-2964-0>.
- Cardona-Olarte, P., Twilley, R.R., Krauss, K.W., Rivera-Monroy, V., 2006. Responses of neotropical mangrove seedlings grown in monoculture and mixed culture under treatments of hydroperiod and salinity. *Hydrobiologia* 569, 325–341. <http://dx.doi.org/10.1007/s10750-006-0140-1>.
- Crist, E.P., 1985. A TM Tasseled Cap equivalent transformation for reflectance factor data. *Remote Sens. Environ.* 17, 301–306. [http://dx.doi.org/10.1016/0034-4257\(85\)90102-6](http://dx.doi.org/10.1016/0034-4257(85)90102-6).
- Dahanayaka, D.D.G.L., Tonooka, H., Minato, A., Ozawa, S., 2013. Monitoring Mangrove Distribution and Changes in Mekong Delta, Vietnam Using Remote Sensing Approach. *IEEE IGARSS 2001–2004*. <http://dx.doi.org/10.1109/IGARSS.2013.6723092>.
- Davis, J.H., 1940. *The Ecology and Geologic Role of Mangroves in Florida*. Carnegie Institution of Washington, Washington, DC, 303–412.
- Eidam, E.F., Nittrouer, C.A., Ogston, A.S., DeMaster, D.J., Liu, J.P., Nguyen, T.T., Nguyen, T.N., in this issue. Dynamic controls on shallow clinoform geometry: Mekong Delta, Vietnam. *Cont. Shelf Res.* Manuscript submitted for publication.
- Ellison, A., 2000. Mangrove restoration: do we know enough? *Restor. Ecol.* 8, 219–229.
- Fricke, A.T., Nittrouer, C., Ogston, A.S., Vo-Luong, H.P., in this issue. Asymmetric progradation of a coastal mangrove forest, Cù Lao Dung, Vietnam. *Cont. Shelf Res.* Manuscript submitted for publication.
- Gao, J., 1998. A hybrid method toward accurate mapping of mangroves in a marginal habitat from spot multispectral data. *Int. J. Remote Sens.* 19, 1887–1899. <http://>

- [dx.doi.org/10.1080/014311698215045](https://doi.org/10.1080/014311698215045).
- Gebhardt, S., Gebhardt, S., Nguyen, L.D., Kuenzer, C., 2012. The Mekong Delta System. <https://doi.org/10.1007/978-94-007-3962-8>.
- Giri, C., Ochieng, E., Tieszen, L.L., Zhu, Z., Singh, A., Loveland, T., Masek, J., Duke, N., 2011. Status and distribution of mangrove forests of the world using earth observation satellite data. *Glob. Ecol. Biogeogr.* 20, 154–159. <https://doi.org/10.1111/j.1466-8238.2010.00584.x>.
- Google Earth, 2016. v 7.1.2.2041, January 25, 2015. Cù Lao Dung Island, Vietnam. 9°31'14.22" N, 106°16'39.11" E, Eye alt 21888 ft. Astrium 2016. June 10.
- Henderson, St., Benjamin, N., Mullarney, J., & Bryan, K., in this issue. Wave-frequency flows within a near-bed vegetation canopy. *Cont. Shelf Res.* Manuscript submitted for publication.
- Kasawani, I., Norsalizi, U., Mohdhasmadi, I., 2010. Analysis of spectral vegetation indices related to soil-line for mapping mangrove forests using satellite imagery. *Appl. Remote Sens.* J. 1, 31–35.
- Kennedy, R.E., Yang, Z., Cohen, W.B., 2010. Detecting trends in forest disturbance and recovery using yearly Landsat time series: 1. LandTrendr - Temporal segmentation algorithms. *Remote Sens. Environ.* 114, 2897–2910. <https://doi.org/10.1016/j.rse.2010.07.008>.
- Kuenzer, C., Bluemel, A., Gebhardt, S., Quoc, T.V., Dech, S., 2011. Remote sensing of mangrove ecosystems: a review. *Remote Sens.* <https://doi.org/10.3390/rs3050878>.
- Lewis, R.R., 2005. Ecological engineering for successful management and restoration of mangrove forests. *Ecol. Eng.* 24, 403–418. <https://doi.org/10.1016/j.ecoleng.2004.10.003>.
- Li, Z., Saito, Y., Mao, L., Tamura, T., Li, Z., Song, B., Zhang, Y., Lu, A., Sieng, S., Li, J., 2012. Mid-Holocene mangrove succession and its response to sea-level change in the upper Mekong River delta, Cambodia. *Quat. Res.* 78, 386–399. <https://doi.org/10.1016/j.yqres.2012.07.001>.
- Liao, B., Zheng, D., Zheng, S., 1998. The studies on seedling nursery and afforestation techniques of *Aegiceras corniculatum* of mangroves. *For. Res.* 11, 480–486.
- Long, J.B., Giri, C., 2011. Mapping the Philippines' mangrove forests using Landsat imagery. *Sensors* 11, 2972–2981. <https://doi.org/10.3390/s110302972>.
- Lugo, A., Snedaker, S., 1974. The ecology of mangroves. *Annu. Rev. Ecol. Syst.* 5, 39–64.
- Brander, M., Wagtendonk, A. L., J., S. Hussain, S., McVittie, A., Verburg, P.H., de Groot, R.S., van der Ploeg, S., 2012. Ecosystem service values for mangroves in Southeast Asia: a meta-analysis and value transfer application. *Ecosyst. Serv.* 1, 62–69. <https://doi.org/10.1016/j.ecoser.2012.06.003>.
- Marchand, M., 2008. Mangrove restoration in Vietnam: Key considerations and a practical guide.
- Masek, J.G., Vermote, E.F., Saleous, N., Wolfe, R., Hall, F.G., Huemmrich, F., Gao, F., Kutler, J., Lim, T.K., 2012. LEDAPS Landsat calibration, reflectance, atmospheric correction preprocessing code. <https://doi.org/10.3334/ORNLDAAAC/108>.
- McKee, K., 1993. Soil physicochemical patterns and mangrove species distribution - reciprocal effects? *J. Ecol.* 81, 477–487.
- Myint, S.W., Giri, C.P., Wang, L., Zhu, Z., Gillette, S.C., 2008. Identifying mangrove species and their surrounding land use and land cover classes using an object-oriented approach with a lacunarity spatial measure. *GIScience Remote Sens.* 45, 188–208. <https://doi.org/10.2747/1548-1603.45.2.188>.
- Nardin, W., Locatelli, S., Pasquarella, V., Rulli, M.C., Woodcock, C.E., Fagherazzi, S., 2016a. Dynamics of a fringe mangrove forest detected by Landsat images in the Mekong River Delta, Vietnam. *Earth Surf. Process. Landf.* 41, 2024–2037. <https://doi.org/10.1002/esp.3968>.
- Nardin, W., Woodcock, C.E., Fagherazzi, S., 2016b. Bottom sediments affect *Sonneratia* mangrove forests in the prograding Mekong delta, Vietnam. *Estuar. Coast. Shelf Sci.* 177, 60–70. <https://doi.org/10.1016/j.ecss.2016.04.019>.
- Nguyen, H.N., 2007. Human development report 2007 / 2008 flooding in Mekong River Delta, Viet Nam. *Hum. Dev. Rep.* 4.
- Norris, B., Mullarney, J., Bryan, K., & Henderson, S., in this issue. The effect of pneumatophore density on turbulence: a field study in a *Sonneratia*-dominated mangrove forest, Vietnam. *Cont. Shelf Res.* Manuscript submitted for review.
- The Orfeo Toolbox [Computer software], 2015. Retrieved from (<https://www.orceo-toolbox.org>).
- Piou, C., Feller, I.C., Berger, U., Chi, F., Piou, C., 2006. Zonation patterns of Belizean offshore mangrove forests 41 years after a catastrophic hurricane. *Biotropica* 38, 365–374.
- Quoc Vo, T., Kuenzer, C., Oppelt, N., 2015. How remote sensing supports mangrove ecosystem service valuation: a case study in Ca Mau province, Vietnam. *Ecosyst. Serv.* 14, 67–75. <https://doi.org/10.1016/j.ecoser.2015.04.007>.
- Ren, H., Shuguang, J., Lu, H., Qianmei, Z., Weijun, S., 2008. Restoration of mangrove plantations and colonization by native species in Leizhou bay, South China. *Ecol. Res.* 23, 401–407. <https://doi.org/10.1007/s11284-007-0393-9>.
- Richards, D.R., Friess, D.A., 2015. Rates and drivers of mangrove deforestation in Southeast Asia, 2000–2012. *Proc. Natl. Acad. Sci.*, 201510272. <https://doi.org/10.1073/pnas.1510272113>.
- Robertson, A.I., Daniel, P.A., Dixon, P., 1991. Mangrove forest structure and productivity in the Fly River estuary, Papua New Guinea. *Mar. Biol.* 111, 147–155. <https://doi.org/10.1007/BF01986356>.
- San, H.T., 1993. Mangroves of Vietnam 7th ed.. IUCN, Bangkok, Thailand.
- Snedaker, S.C., 1982. Mangrove species zonation: why. *Tasks Veg. Sci.* 2, 111–125.
- Son, N.T., Thanh, B.X., Da, C.T., 2016. monitoring mangrove forest changes from multi-temporal Landsat data in Can Gio Biosphere Reserve, Vietnam. *Wetlands*. <https://doi.org/10.1007/s13157-016-0767-2>.
- Thom, B., 1967. Mangrove ecology and deltaic geomorphology: Tabasco, Mexico. *J. Ecol.* 55, 301–343.
- Tomlinson, P.B., 1986. *The Botany of Mangroves*. Cambridge University Press, Cambridge, UK.
- Tong, P.H.S., Auda, Y., Populus, J., Aizpuru, M., Habshi, a.Al, Blasco, F., 2004. Assessment from space of mangroves evolution in the Mekong Delta, in relation to extensive shrimp farming. *Int. J. Remote Sens.* 25, 4795–4812. <https://doi.org/10.1080/01431160412331270858>.
- Tran Thi, V., Tien Thi Xuan, A., Phan Nguyen, H., Dahdouh-Guebas, F., Koedam, N., 2013. Application of remote sensing and GIS for detection of long-term mangrove shoreline changes in Mui Ca Mau, Vietnam. *Biogeosciences* 11, 3781–3795. <https://doi.org/10.5194/bg-11-3781-2014>.
- van Loon, A.F., Dijkema, R., van Mensvoort, M.E.F., 2007. Hydrological classification in mangrove areas: a case study in Can Gio, Vietnam. *Aquat. Bot.* 87, 80–82. <https://doi.org/10.1016/j.aquabot.2007.02.001>.
- Van, T.T., Wilson, N., Thanh-Tung, H., Quisthoudt, K., Quang-Minh, V., Xuan-Tuan, L., Dahdouh-Guebas, F., Koedam, N., 2015. Changes in mangrove vegetation area and character in a war and land use change affected region of Vietnam (Mui Ca Mau) over six decades. *Acta Oecologica* 63, 71–81. <https://doi.org/10.1016/j.actao.2014.11.007>.
- Verbesselt, J., Hyndman, R., Newnham, G., Culvenor, D., 2010. Detecting trend and seasonal changes in satellite image time series. *Remote Sens. Environ.* 114, 106–115. <https://doi.org/10.1016/j.rse.2009.08.014>.
- Warner, R., Kaidonis, M., Dun, O., Rogers, K., Shi, Y., Nguyen, T.T.X., Woodroffe, C.D., 2016. Opportunities and challenges for mangrove carbon sequestration in the Mekong River Delta in Vietnam. *Sustain. Sci.* <https://doi.org/10.1007/s11625-016-0359-3>.
- Watson, J.D., 1928. Mangrove forests of the Malay Peninsula. *Malay. For. Rec.* 6, 1–275.
- Wolcke, J., Albers, T., Roth, M., Vorlaufer, M., Korte, A., 2015. Integrated coastal protection and mangrove belt rehabilitation in the Mekong Delta.
- Woodroffe, C., 1992. Mangrove sediments and geomorphology. *Trop. Mangrove Ecosyst.* 7–41.
- Wyatt, A., Thanh, N., Gian, T., 2012. Viet Nam Situation Analysis. Retrieved from (<https://www.iucn.org>).
- Zhu, Z., Woodcock, C., 2012. Object-based cloud and cloud shadow detection in Landsat imagery. *Remote Sens. Environ.* 118, 83–94. <https://doi.org/10.1016/j.rse.2011.10.028>.
- Zhu, Z., Woodcock, C.E., Olofsson, P., 2012. Continuous monitoring of forest disturbance using all available landsat imagery. *Remote Sens. Environ.* 122, 75–91. <https://doi.org/10.1016/j.rse.2011.10.030>.